

Monomer Consumption Rates During Gelation at Various Temperatures: A Fast Transient Fluorescence Study

Ö. PEKCAN, D. KAYA

Istanbul Technical University, Department of Physics, Maslak, 80626 Istanbul, Turkey

Received 4 May 2000; accepted 30 October 2000

ABSTRACT: The gelation during free-radical crosslinking copolymerization (FCC) of methyl methacrylate (MMA) and ethylene glycol dimethacrylate (EGDM) was studied by using fast transient fluorescence (FTRF) technique. Pyrene (Py) was used as a probe for the FTRF experiments. Fluorescence lifetimes of Py from its decay traces were measured and used to monitor the gelation process at various temperatures. MMA consumption rates were measured during gelation process by using the Stern–Volmer model. Gelation activation energy ΔE_G was measured and found to be 15.6 kcal mol⁻¹. © 2001 John Wiley & Sons, Inc. *J Appl Polym Sci* 81: 3161–3168, 2001

Key words: fast transient fluorescence; lifetimes; gelation activation energy

INTRODUCTION

Because of its long, excited singlet lifetime, pyrene (Py) as a chromophore¹ is an attractive choice for studying dynamics in polymers. Py has been successfully employed as the fluorescence probe in the study of micellar² and phospholipid dispersion.³ These studies focus on the use of dynamics of quenching of Py monomer fluorescence and excimer formation processes. The other application of the use of Py as a fluorescence probe is the study of the vibronic fine structure of its monomer fluorescence. The intensities of the various vibronic bands show a strong dependence on the solvent environment.⁴ In the presence of polar solvents, there is an enhancement in the intensity of the 0–0 band, whereas there is a little effect on other bands; thus, the ratio of intensities of these bands has been used to study environmental change. For about two decades, the transient fluorescence (TRF) technique used for measuring fluorescence decay was routinely applied to study many polymeric systems using dyes both

as a probe and/or as labels.^{5–9} TRF spectroscopy with direct energy transfer (DET) and quenching method was used to characterize internal morphologies of composite polymeric materials.^{10,11} Quenching besides DET is the general word used to describe any bimolecular process, which decreases the emission decay rate. The most important feature of these quenching mechanisms involves interactions between groups over different interaction distances. A single-photon counting (SPC) technique, which produces decay curves and measures lifetimes in conjunction with DET, was used to study the diffusion of small dye molecules within the interphase domain of anthracene and/or phenanthrene-labeled poly(methyl methacrylate) (PMMA) particles.¹²

Free-radical crosslinking copolymerization (FCC) was widely used to synthesize polymer gels. Several theories were developed in the past half century to describe gel formation in FCC, among which percolation theory provides a basis for modeling sol–gel phase transition.^{13–15} The percolation models based on simulation in *n*-dimensional space can predict critical exponents or gel fraction, weight-averaged degree of polymerization, radius of gyration, etc., near the sol–gel phase transition called the critical region. This

Correspondence to: Ö. Pekcan.

Journal of Applied Polymer Science, Vol. 81, 3161–3168 (2001)
© 2001 John Wiley & Sons, Inc.

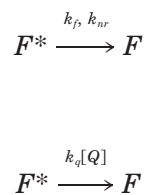
theory is, however, unrealistic outside of this region due to the difficulty of the introduction of realistic mobilities. Another type of theories is called the mean-field theories, such as the statistical and kinetic theories based on a tree approximation. Statistical theories originate from Flory¹⁶ and Stockmayer¹⁷ and assume equal reactivities of functional groups and the absence of cyclization reactions. The critical exponents in percolation theory differ from those found in Flory–Stockmayer. In FCC, the formation of bonds building the network can be described by using differential equations with reaction time or monomer conversion as the independent variable. The kinetic approaches can take into account all the kinetic features of copolymerization and crosslinking reactions that may suggest a more realistic approach to the mechanism of gelation process.^{18–21} Kinetic models have been extensively used to describe the relations among the molecular weight of polymer and the conversion or reaction time during crosslinking process. In the classical kinetic theory, the rate constant is proportional to the product of the number of functional groups in each reactant. Modification of the classical kinetic theory by using rate constants that also depend on the structural features of the reactants was done.²²

Py derivative was used as a fluorescence molecule to monitor the polymerization, aging, and drying of aluminosilicate gels.²³ These results were interpreted in terms of the chemical changes occurring during the sol–gel process and the interactions between the chromophores and the sol–gel matrix. We reported *in situ* observations of the sol–gel phase transition in free-radical crosslinking copolymerization by using the steady-state fluorescence (SSF) technique.^{24–29} The bond percolation model was employed to obtain some critical exponents during sol–gel transitions of such a system. Recently, fast transient fluorescence (FTRF) technique was used to study dissolution of polymer films and swelling of gels in our laboratory.^{30–32} In this work, the strobe technique of FTRF was used to study sol–gel transition in FCC of methyl methacrylate (MMA) and ethylene glycol dimethacrylate (EGDM) at various temperatures. Gelation activation energy ΔE_G was measured in this temperature range by employing the Stern–Volmer model. *In situ* FTRF experiments were carried out at each temperature by illuminating the sample cell, and fluorescence decay traces were observed by using the Strobe master system (SMS) during gelation.

FLUORESCENCE QUENCHING

Fluorescence intensities of aromatic molecules are affected by both radiative and nonradiative processes.³³ If the possibility of perturbation due to oxygen is excluded, the radiative probabilities are found to be relatively independent of environment and even of molecular species. Environmental effects on nonradiative transitions that are primarily intramolecular in nature are believed to arise from a breakdown of the Born–Oppenheimer approximation.³⁴ The role of the solvent in such a picture is to add the quasi-continuum of states needed to satisfy energy resonance conditions. The solvent acts as an energy sink for rapid vibrational relaxation that occurs after the rate limiting transition from the initial state. Years ago, Birks et al. studied the influence of solvent viscosity on fluorescence characteristics of Py solutions in various solvents and observed that the rate of monomer internal quenching is affected by solvent quality.³⁵ Weber et al. reported the solvent dependence of energy trapping in phenanthrene block polymers and explained the decrease in fluorescence yield with the static quenching, caused by the solvent-induced trapping states.³⁶ A matrix that changes little with temperature will enable the study of molecular properties without changing environmental influence. PMMA was used as such a matrix in many studies.³⁷

Emission of the fluorescence is the radiative transition of an electronically excited molecule from its singlet excited state to its ground state.¹ Fluorescence quenching normally refers to any bimolecular process between the excited singlet state of a fluorescence dye and the second species that enhances the decay rate of the excited state. One can schematically represent the process as



where F and F^* represent the fluorescent molecule and its excited form, and Q is the quencher. k_f , k_{nr} , and k_q represent the fluorescence, nonradiative, and quenching rate constants, respectively. Many types of processes lead to quenching.

Kinetically, the quenching process can be divided into two main categories: dynamic and static. In dynamic quenching, diffusion to form an encounter pair during the excited state lifetime of the dye leads to quenching. In static quenching, diffusion does not occur (which is out of our interest). Dynamic quenching is most likely to occur in fluid solution, where the dye or quencher is free to move. If the quenching rate can be characterized in terms of a single-rate coefficient (k_q) and the unquenched decay rate of F , in terms of a unique lifetime, τ_0 , then the quenching kinetics will follow the Stern–Volmer equation as follows:

$$\tau^{-1} = \tau_0^{-1} + k_q[Q] \quad (1)$$

Here $[Q]$ represents the quencher concentration, and k_q is given by following relation

$$k_q = 4\pi N_A D R 10^{-3} \quad (2)$$

In eq. (2), D is the sum of the mutual diffusion coefficients of the dye and quencher that is inversely dependent on the viscosity of the medium via Stoke–Einstein relation.¹ R presents the sum of their interaction radii and N_A is Avogadro's number.

EXPERIMENTAL

EGDM was commonly used as a crosslinker in the synthesis of polymeric networks. Here, for our use, the monomers MMA (Merck, Germany) and EGDM (Merck) were freed from the inhibitor by shaking with a 10% aqueous KOH solution, washing with water, and drying over sodium sulfate. They were then distilled under reduced pressure over copper chloride. The initiator, 2,2'-azobisisobutyronitrile (AIBN; Merck), was recrystallized twice from methanol. Here EGDM (0.025%) and AIBN (0.26 wt %) was dissolved in MMA and this solution was transferred into round quartz cells of 10-mm internal diameter for fluorescence decay measurements.

The use of *in situ* FTRF technique monitored gelation in FCC of MMA and EGDM. The radical copolymerization of MMA and EGDM was performed in bulk in the presence of AIBN as an initiator at four different temperatures (50, 55, 60, and 65°C). Py lifetimes were measured to detect the gelation process where MMA act as an energy sink for the excited Py molecules. The

PMMA network, however, provides an ideal, unchanged environment for the excited Py molecules. Naturally, from these experiments one may expect a drastic increase in Py lifetimes during gelation process.

In situ fluorescence decay experiments from which Py lifetimes can be determined were performed by using Photon Technology International's (PTI) SMS. In the strobe, or pulse sampling technique,³⁸ the sample is excited with a pulse light source. The name comes about because the PMT is gated or strobed by a voltage pulse that is synchronized with the pulsed light source. The intensity of fluorescence emission is measured in a very narrow time window on each pulse and saved in a computer. The time window is moved after each pulse. The strobe has the effect of turning of the PMT and measuring the emission intensity over a very short time window. When the data was sampled over the appropriate range of time, a decay curve of fluorescence intensity versus time can be constructed. Because the strobe technique is intensity-dependent, the strobe instrument is much faster than SPC and even faster than phase instrument. Strobe instrument is much simpler to use than SPC and the data are easier to interpret than the phase system. Because of these advantages, SMS is used to monitor gelation processes, which take a few hours.

All lifetime measurements were made at a 90° position and slit widths were kept at 10 nm. The gelation experiment was performed in a round quartz cell at a given temperature which was placed in the SMS and fluorescence decay was collected over three decades of decay. The sample was then illuminated with 345-nm excitation light and Py fluorescence emission was detected at 395 nm. The uniqueness of the fit of the data to the model is determined by χ^2 ($\chi^2 < 1.20$), the distribution of weighted residuals, and the autocorrelation of the residuals. All samples were deoxygenated by bubbling nitrogen for 10 min.

RESULTS AND DISCUSSION

Figure 1 presents the fluorescence decay profiles of Py in various gelation steps at 50°C. It is observed that as the gelation time t_g is increased, excited Py's decay slower and slower by indicating that quenching of excited Py's decrease. To monitor gelation processes, the fluorescence decay curves are measured and were fitted to the equation

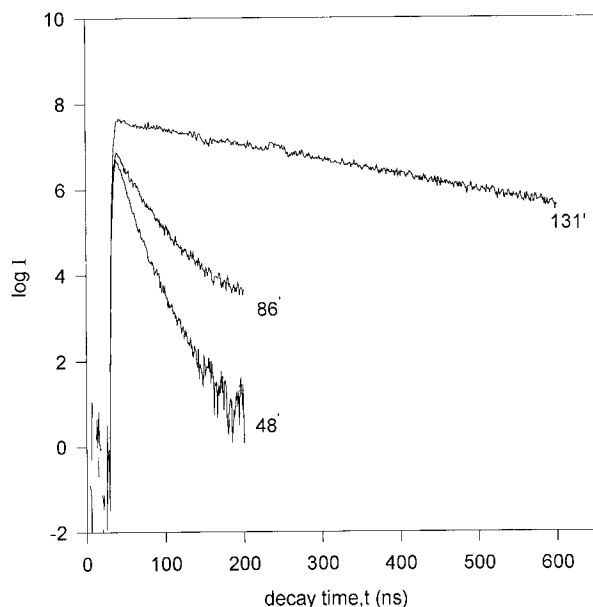


Figure 1 Fluorescence decay profiles of excited Py, in various gelation steps at 50°C. I is the Py intensity. Numbers on each curve present the gelation times in minutes.

$$I = I_0 \exp(-t/\tau) \quad (3)$$

where I and I_0 are the intensity of Py at time t and 0 and τ is the lifetime of Py. Decay curve and its fit to eq. (3) are shown in Figure 2 for the gelation step in 131' at 50°C. τ values were produced at each gelation step by using the linear least-squares analysis. τ values obtained during sol-gel phase transition are plotted versus t_g in Figure 3a–3d for the temperatures of 50, 55, 60, and 65°C, respectively. As seen in Figure 3, Py lifetimes τ increased drastically from very low values (10 ns) to their unquenched (τ_0) value during gelation at each temperature. The onset of gelation time (t_0) decreased as the gelation temperature is increased, indicating an early gelation process takes place at high temperatures. To quantify these results, a Stern–Volmer type of quenching mechanism is proposed for the fluorescence decay of Py during gelation process, where eq. (1) can be employed and rewritten as follows:

$$\tau^{-1} = \tau_0^{-1} + k_q[\text{MMA}] \quad (4)$$

Here it is assumed that MMA is the only quencher for the excited Py molecules. τ_0 values between 300 and 250 ns are chosen at $t_g = 120$ and 80 min, where the gelation is completed and

the ideal solid network is reached for the corresponding samples. Because MMA is the only quencher for Py by knowing the $[\text{MMA}_0]$ value as 9.4M, k_q is measured before the polymerization has started and found to be $9.14 \times 10^6 \text{M}^{-1} \text{s}^{-1}$. Here it is assumed that k_q stays constant for a given temperature and viscosity during polymerization and a decrease in $[\text{MMA}]$ results in an increase in τ values according to eq. (4). In other words, the quenching process takes place in the MMA environment where D and R values in eq. (2) do not vary during polymerization. By using the k_q value and the measured τ values during the gelation process, $[\text{MMA}]$ values are obtained from eq. (4). A naive model³⁹ for quick interpretation of the behavior of $[\text{MMA}]$ versus gelation time t_g can be employed, where the first step in free-radical polymerization is the decomposition of the initiator molecule with the rate constant k_i into two species carrying unpaired electrons called free

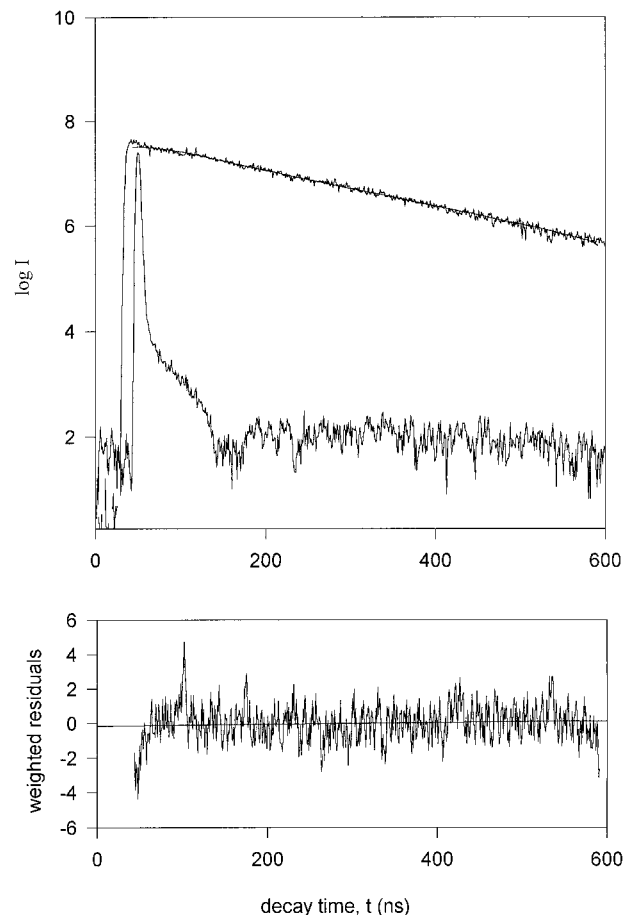


Figure 2 The fit of the decay curve of Py according to eq. (2), at the gelation time of 103' at 50°C. The sharp, peaked curve is the lamp profile.

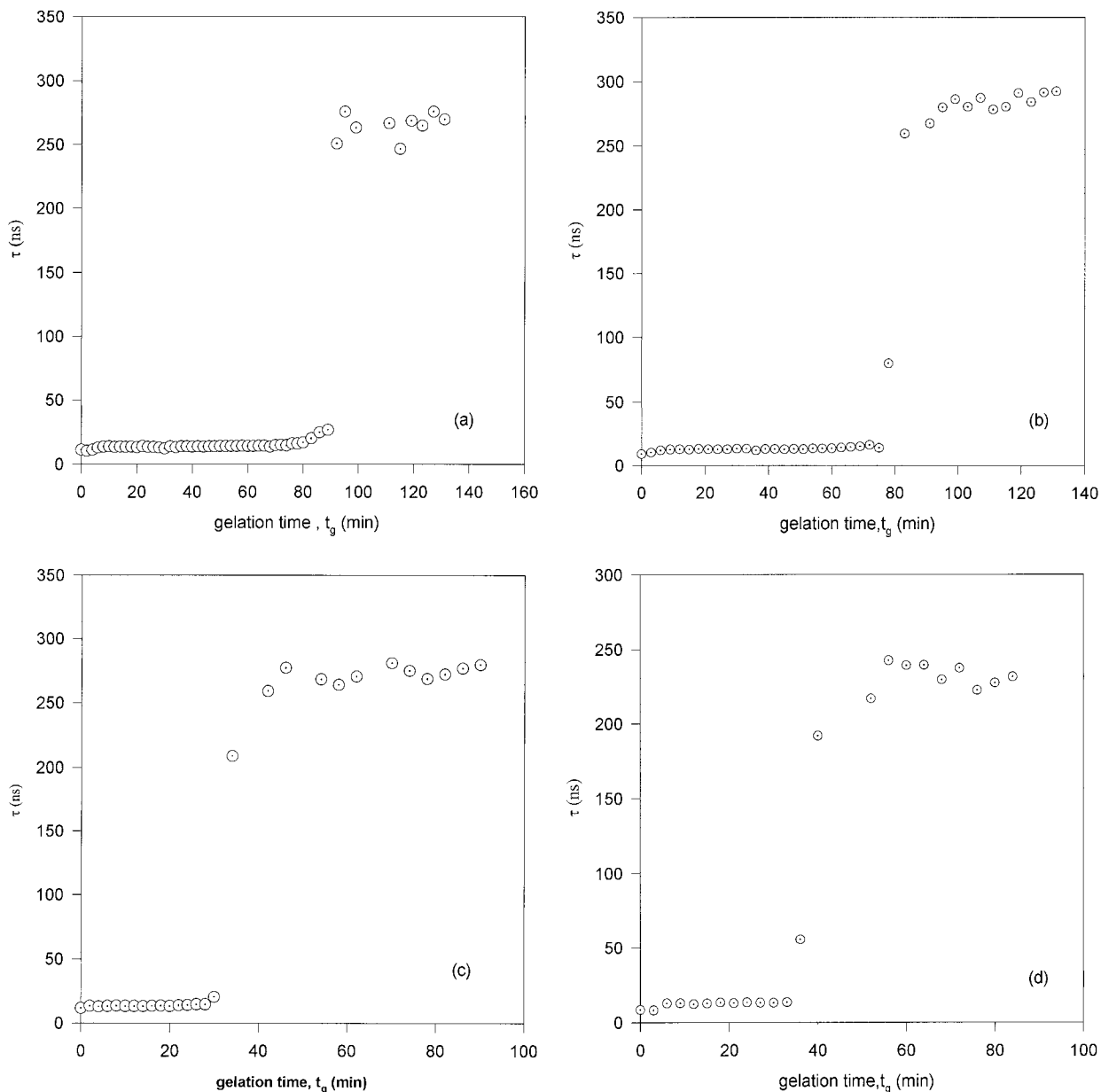


Figure 3 Plot of the Py lifetimes τ versus gelation time t_g for the gelation temperatures of (a) 50, (b) 55, (c) 60, (d) 65°C.

radicals. A free radical can then react to open the double bond of a vinyl monomer and add to it, with one electron remaining unpaired. In a very short time, usually a few seconds or less, many more monomers add successively to the growing chain with the propagation rate constant k_p . Finally, two radicals react to end each other's growth activity and form one or more polymer molecules. This bimolecular process is called termination reaction and is identified with the rate constant k_t . During the FCC, addition of divinyl

monomers to the growing chain results in the formation of polymer molecules with reactive sites (pendant vinyl groups). These reactive sites on polymer chains offer the possibility of forming chemical structures of macroscopic dimensions called polymer gels. The rate of consumption of monomer is usually called the rate of polymerization

$$\frac{d[M]}{dt} = -k_r[M] \quad (5)$$

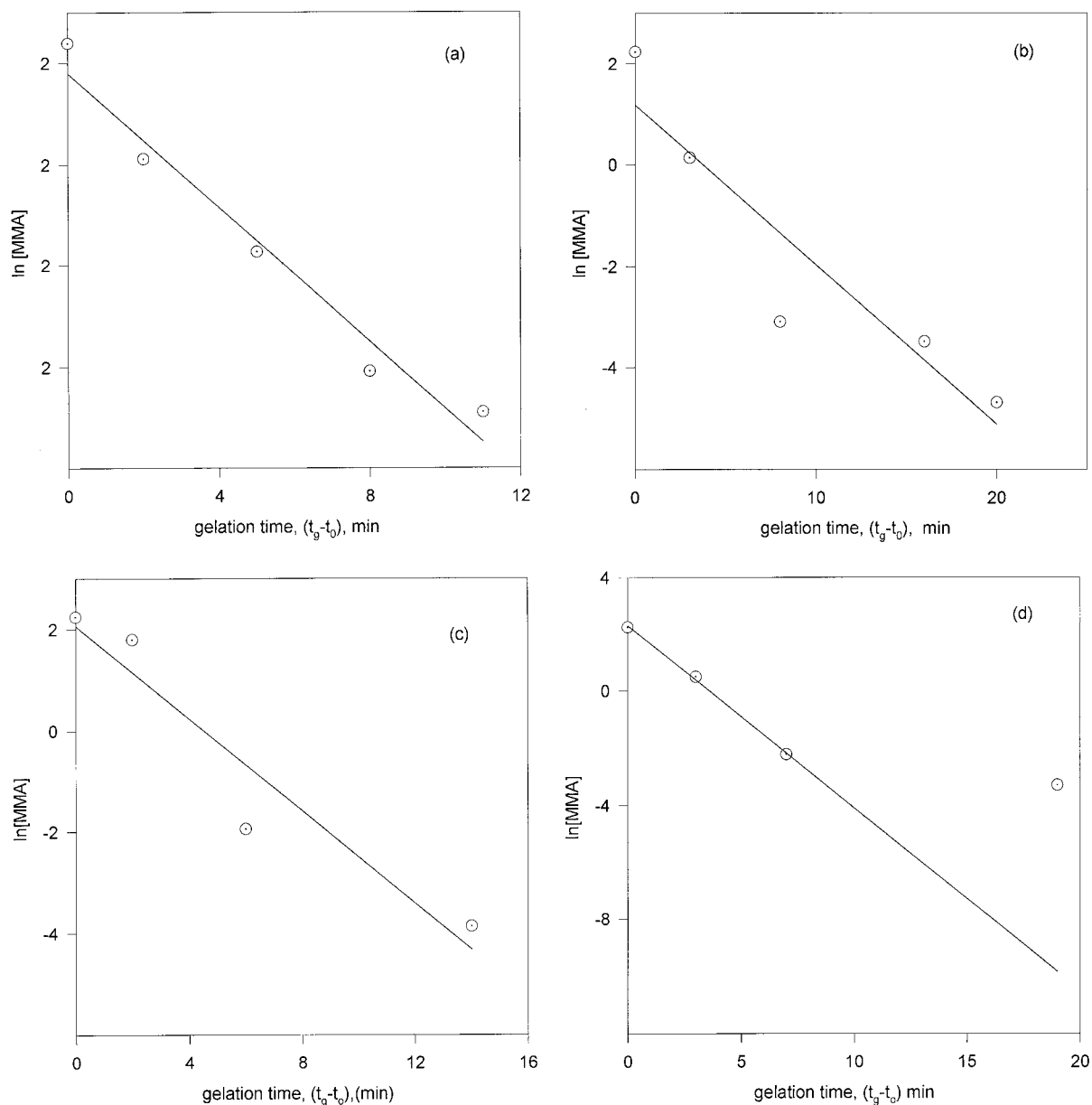


Figure 4 The fit of the data in Figure 3 according to eq. (5). The slope of the linear relations produces the composite rate constants k_r for the polymerization of MMA at (a) 50, (b) 55, (c) 60, (d) 65°C.

which is applied only under steady-state conditions. Here $[M]$ is the concentration of monomer, and k_r is the composite rate constant, which is composed of k_p , k_i , and k_t rates.³⁹ The solution of the eq. (5) produces the relation for the monomer consumption as follows

$$[M] = [M_0]\exp(-k_r t) \quad (6)$$

where $[M_0]$ is the concentration of monomer at $t = 0$.

The produced $[MMA]$ consumption curves versus t_g obey the relation in eq. (6). The logarithmic form of $[MMA]$ versus $(t_g - t_0)$ are plotted in Figure 4a–4d for samples polymerized at 50, 55, 60, and 65°C, where t_0 is the onset of gelation time which corresponds to $[MMA_0]$ value. In Figure 4, the slope of the linear relations produce the composite rate constants k_r according to eq. (6), for polymerizations

during gelation at various temperatures. It is observed that, as the temperature is raised, the composite rate constant increases as expected. A simple Arrhenius treatment to this data in Figure 5 produces the gelation activation energy ΔE_G as 15.6 kcal mol⁻¹ for this given temperature range. Here in the following relation

$$k_r = k_{r,0} \exp(-\Delta E_G/kT) \quad (7)$$

$k_{r,0}$ is the composite rate constant at infinite temperature, and k is the Boltzmann constant.

Similar Arrhenius treatment can also be made for the onset of gelation time t_0 as

$$t_0^{-1} = t_{00}^{-1} \exp(-\Delta E'_G/kT) \quad (8)$$

where t_{00} is the t_0 at infinite temperature and $\Delta E'_G$ is the gelation activation energy. In Figure 6, the logarithmic plot of t_0^{-1} versus inverse temperature is presented where the slope of the linear relation produced the $\Delta E'_G$ value as 15.9 kcal mol⁻¹, which is very close to the ΔE_G value. From here, one may conclude that both rates of eqs. (7) and (8) produce similar gelation activation energy, which is also very close to the our early findings for the FCC process during bulk polymerization of MMA.²⁵

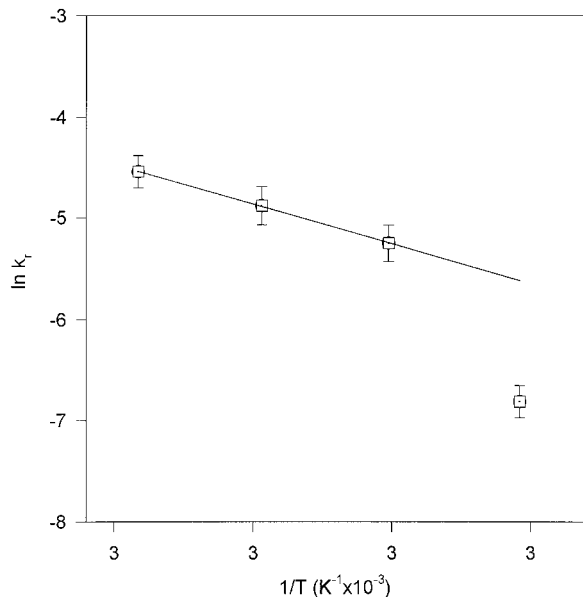


Figure 5 Logarithmic plot of composite rate constant k_r versus inverse gelation temperature T according to Arrhenius relation as $k_r = k_{r,0} \exp(-\Delta E_G/kT)$. Here ΔE_G is the gelation activation energy.

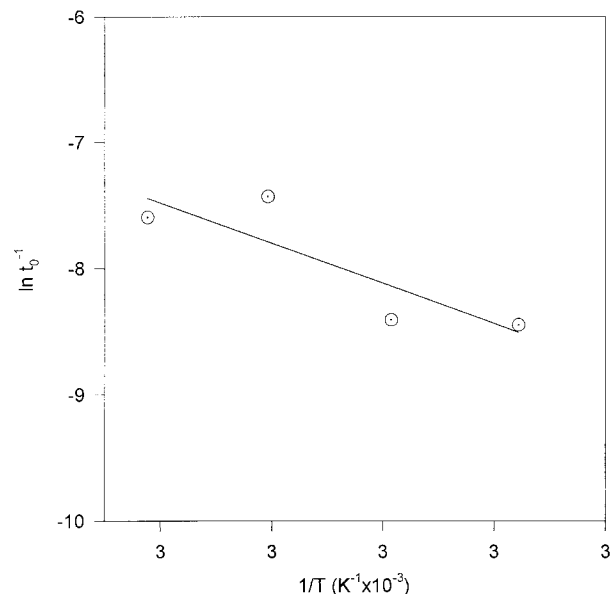


Figure 6 Logarithmic plot of onset of gelation time t_0 versus inverse temperature T according to Arrhenius relation as $t_0^{-1} = t_{00}^{-1} \exp(-\Delta E'_G/kT)$. Here $\Delta E'_G$ is the gelation activation energy.

In summary, a novel technique (FTRF) was introduced in this work which could measure the gelation activation energy quite satisfactorily. Because FTRF measures lifetimes with no art effects, the results are more reliable compared to intensity measurements. However, more points are needed in Figure 3 to be more accurate for measuring k_r values.

REFERENCES

1. Birks, J. B. *Photophysics of Aromatic Molecules*; Wiley-Interscience: New York, 1971.
2. Dorrance, R. C.; Hunda, T. F. *J Chem Soc, Faraday Trans* 1972, 68, 1312.
3. Cheng, S.; Thomas, J. K. *Radiat Res* 1974, 60, 268.
4. Kalyanasundaram, K.; Thomas, J. K. *J Am Chem Soc* 1977, 99, 2039.
5. Pekcan, Ö.; Winnik, M. A.; Croucher, M. D. *Macromolecules* 1983, 16, 669.
6. Pekcan, Ö.; Winnik, M. A.; Croucher, M. D. *J Polym Sci, Polym Lett Ed* 1983, 21, 1011.
7. Pekcan, Ö.; Winnik, M. A.; Croucher, M. D. *Phys Rev Lett* 1988, 61, 641.
8. Pekcan, Ö.; Egan, L. S.; Winnik, M. A.; Croucher, M. D. *Macromolecules* 1990, 23, 2210.
9. Pekcan, Ö. *Chem Phys Lett* 1992, 20, 198.
10. Winnik, M. A. in *Polymer Surfaces and Interfaces*; Feast, J.; Munro, H., Eds., Wiley: London, 1983; Chapter 1.

11. Winnik, M. A.; Pekcan, Ö.; Chen, L.; Croucher, M. D. *Macromolecules* 1988, 21, 55.
12. Pekcan, Ö. *J Appl Polym Sci* 1996, 59, 521.
13. Stauffer, D. *Introduction to Percolation Theory*; Taylor and Francis: London, 1985.
14. Stauffer, D.; Coniglio, A.; Adam, M. *Adv Polym Sci* 1982, 44, 103.
15. Herrmann, H. *J Phys Rev* 1986, 153, 136.
16. Flory, P. J. *J Am Chem Soc* 1941, 63, 3083.
17. Stockmayer, W. H. *J Chem Phys* 1943, 11, 45.
18. Mikos, A. G.; Takoudis, C. G.; Peppas, N. A. *Macromolecules* 1986, 19, 2174.
19. Tobita, H.; Hamielec, A. E. *Macromolecules* 1989, 22, 3098.
20. Batch, G. L.; Macosko, C. W. *J Appl Polym Sci* 1992, 44, 1711.
21. Okay, O. *Polymer* 1994, 35, 796.
22. Dusek, K. *J Macromol Sci, Chem A* 1991, 28, 843.
23. Panxviel, J. C.; Dunn, B.; Zink, J. J. *J Phys Chem* 1994, 93, 2134.
24. Pekcan, Ö.; Yilmaz, Y.; Okay, O. *Chem Phys Lett* 1994, 229, 537.
25. Yilmaz, Y.; Pekcan, Ö.; Okay, O. *Polymer* 1996, 37, 2049.
26. Pekcan, Ö.; Yilmaz, Y.; Okay, O. *J Appl Polym Sci* 1996, 61, 2279.
27. Pekcan, Ö.; Yilmaz, Y. *Prog Colloid Polym Sci* 1996, 102, 89.
28. Pekcan, Ö.; Yilmaz, Y.; Okay, O. *Polymer* 1997, 38, 1693.
29. Yilmaz, Y.; Erzan, A.; Pekcan, Ö. *Phys Rev E: Stat Phys, Plasmas, Fluids, Relat Interdiscip Top* 1998, 58, 7487.
30. Pekcan, Ö.; Ugur, S. *J Appl Polym Sci* 1999, 74, 984.
31. Ugur, S.; Pekcan, Ö. *Polymer* 2000, 41, 1571.
32. Pekcan, Ö.; Kaya, D.; Erdogan, M. *J Polym Sci* to appear.
33. Kropp, L. J.; Dawson, R. W. *Fluorescence and Phosphorescence of Aromatic Hydrocarbons in Polymethylmethacrylate*; Lim, E. C., Ed.; in *International Conference on Molecular Luminescence*; New York, 1969.
34. Bixon, M.; Jortner, J. *J Chem Phys* 1968, 48, 715.
35. Birks, J. B.; Lumb, M. D.; Munro, I. H. *Proc R Soc London, Ser A* 1964, 277, 289.
36. Kamioka, K.; Weber, S. E.; Morishima, Y. *Macromolecules* 1988, 21, 972.
37. Jones, P. F.; Siegel, S. *J Chem Phys* 1964, 50, 1134.
38. Ware, W. R.; James, D. R.; Siemiarzuck, A. *Rev Sci Instrum* 1992, 63, 1710.
39. Young, R. J. *Introduction to Polymers*; Chapman and Hall: New York, 1983.